Applied Catalysis A: General 475 (2014) 127–133

Contents lists available at ScienceDirect

Applied Catalysis A: General

journal homepage: www.elsevier.com/locate/apcata

Characterization and catalytic performance of modified nano-scale ZSM-5 for the acetone-to-olefins reaction

Hiroki Konno, Teruoki Tago*, Yuta Nakasaka, Gaku Watanabe, Takao Masuda

Division of Chemical Process Engineering, Faculty of Engineering, Hokkaido University, N13 W8, Kita-ku, Sapporo, Hokkaido 060-8628, Japan

ARTICLE INFO

Article history:
Received 22 November 2013
Received in revised form 10 January 2014
Accepted 15 January 2014
Available online 20 January 2014

Keywords:
Acidity modification
Nano-zeolite
ZSM-5
Acetone conversion
Light olefins

ABSTRACT

In the acetone to olefins (ATO) reaction using ZSM-5 zeolites, isobutylene is initially produced via decomposition of an acetone dimer, followed by dimerization of the isobutylene and its cracking to form ethylene and propylene. Nano-scale ZSM-5 zeolite exhibited stable activity during the ATO reaction compared with that of macro-scale ZSM-5. In order to further improve the catalytic stability of the nano-scale ZSM-5, control of the acidity of nano-scale ZSM-5 zeolites through SiO_2 unit formation was examined using phenyl silane and triphenyl silane as new deactivators. This modification led to an increase in the olefins yield and an improvement in the catalyst lifetime. In particular, the regioselective deactivation of acid sites located on the external surface of the zeolite inhibits the formation of aromatics. Moreover, the acidity control within the pores significantly improved the catalyst lifetime. Notably, the modified nano-scale ZSM-5 zeolite exhibited a stable olefins yield above 55 C-mol% for 180 h.

1. Introduction

Light olefins are important basic raw materials for the petrochemical industry, and demand for such products is increasing every year [1–3]. Ethylene, propylene, and isobutylene are key building blocks for the production of chemical products, such as polyethylene (LDPE, HDPE), polypropylene (PP), polyvinyl chloride (PVC), polyacrylonitrile (PAN), ethylene oxide, propylene oxide, methyl methacrylate (MMA), ethyl tertiary-butyl ether (ETBE), and so on. These light olefins are mainly produced by steam cracking of naphtha. However, because this process consumes more than 30% of the total amount of energy required for petrochemical refinement, new efficient processes for light olefins production are required. Promising alternative processes for light olefins production include naphtha catalytic cracking (NCC) [4–11], methanol-to-olefins (MTO) [12–14], ethanol-to-olefins (ETO) [15–17], and propane dehydrogenation (PDH) [18,19].

Because a large amount of acetone is obtained as a by-product in the cumene process [20], we investigated the possibility of light olefins synthesis from acetone (acetone-to-olefins, ATO) over zeolite catalysts, and reported that a high light olefins yield was achieved using ZSM-5 zeolite [21] and an alkali metal ion-exchanged Beta zeolite [22]. In this reaction, isobutylene was first produced from acetone via the formation of an acetone dimer (diacetone alcohol) and trimer (isophorone), followed by production of propylene, ethylene, and aromatics [21–27]. These intermediates are involved in a series of reactions that result in the generation of coke as the terminal product.

Previously, we reported that the use of ZSM-5 zeolite was effective for the suppression of aromatics formation because the consecutive reactions are mainly routed via diacetone alcohol formation/decomposition, rather than isophorone formation/decomposition, which is an aromatics precursor, due to the spatial limitations of ZSM-5 zeolite with its 10-membered rings [21]. However, the undesirable excessive reactions that produce aromatics and coke due to light olefins consumption do readily occur on acid sites near the internal cross-sectional spaces and on the external surfaces of the zeolite crystals. Therefore, a method is desired for the regioselective deactivation and acidity control of the acid sites of zeolite crystals in order to prevent these undesirable excessive reactions.

We previously developed a method for the modification of the acidity of zeolites using organic silane compounds (catalytic cracking of silane, or the CCS method) [28–30]. In the CCS method, SiO_2 units are formed on the acid sites where the silane compounds are chemically adsorbed, thus resulting in modification of the acidity of the zeolite. Because the molecular diameter of the silane compounds depends on the types of organic groups bound to the Si atom, it was anticipated that deactivation of the acid sites located on the external surface of the zeolite crystals could be achieved by utilizing the molecular sieving effect of the zeolites. Furthermore, when silane compounds those are comparable to or smaller in size than the size of the zeolite pores, SiO_2 formation may occur on the

* Corresponding author. Tel.: +81 117066551; fax: +81 117066552.
E-mail address: tago@eng.hokudai.ac.jp (T. Tago).

0926-860X/$ – see front matter © 2014 Elsevier B.V. All rights reserved.
http://dx.doi.org/10.1016/j.apcata.2014.01.031

acid sites located at the cross-sectional spaces within the crystals, leading to further modification of the acidity [30].

Herein, we report the results obtained when triphenyl silane (TPS) and phenyl silane (PS) were used as new deactivators. The modified nano-scale ZSM-5 zeolites prepared using TPS and PS were extensively characterized, and their catalytic performance for the ATO reaction was investigated. The type of Si-compounds used for modification of the acidity was observed to influence the product selectivity. Notably, the PS-treated, nano-scale ZSM-5 showed both high selectivity for light olefins and stable activity during the ATO reaction. The relationship between the acidity modification and the catalytic performance is also discussed.

2. Experimental

2.1. ZSM-5 zeolite preparation

Nano-scale ZSM-5 zeolite was prepared via hydrothermal synthesis using a water/surfactant/organic solvent (emulsion method) [31,32]. An aqueous solution containing the Si and Al source materials was obtained by hydrolyzing each metal alkoxide in a dilute tetrapropyl ammonium hydroxide (TPAOH)/water solution. The water solution (10 ml) thus obtained was added to the surfactant/organic solvent (70 ml, surfactant concentration of 0.5 mol/l). Polyoxyethylene-(15)-oleyl ether and cyclohexane were employed as the surfactant and organic solvent, respectively. The water/surfactant/organic solvent mixture thus obtained was poured into a Teflon-sealed stainless steel bottle and heated to 423 K for 72 h. In order to obtain macro-scale ZSM-5 as a comparative catalyst, hydrothermal synthesis was also carried out without the surfactant/organic solvent (conventional method). The precipitates thus obtained were washed with alcohol, dried at 373 K for 12 h, and calcined at 823 K for 3 h in an air stream. Physically adsorbed and/or ion-exchanged sodium ions on the zeolite surface were removed and exchanged with NH_4^+ using a conventional ion exchange technique with a 10% NH_4NO_3 aqueous solution. The powdered NH_4^+-zeolite described above was pelletized, crushed, and sieved to yield samples ca. 0.3 mm in diameter that were subsequently heated to 823 K to yield an H-ZSM-5 zeolite for the ATO reaction.

2.2. ZSM-5 zeolite acidity control

A ZSM-5 zeolite was exposed to an organic silane compound vapor at 373 K in a nitrogen stream for 2 h, after which time the feed of the organic silane compound was then halted in order to enable the removal of any silane compounds physically adsorbed on the zeolite surface. The sample was then heated to 873 K in order to chemically decompose the silane molecules adsorbed on the acid sites and deposit a silicon-containing carbonaceous residue. The sample was then calcined in an air stream at 873 K, during which time the silicon-containing carbonaceous residue was converted into SiO_2 unit on each acid site, resulting in deactivation. In other words, the SiO_2 units were formed on the acid sites where the silane compounds were chemically adsorbed. Previously, we showed that SiO_2 units can be formed on the acid sites of zeolites using this CCS method, and that the regioselective deactivation of the acid sites is achieved using silane compounds of different molecular sizes [28–30]. In this study, two types of silane compounds were employed for the first time: triphenyl silane (TPS) and phenyl silane (PS). The order for the molecular size of the silane compounds and pore size of an MFI-type zeolite is TPS > pore diameter of MFI ≈ PS. Therefore, in the TPS treatment, because the molecular size of TPS is larger than the pore size of the ZSM-5 zeolite, the acid sites on the outer surface can be selectively deactivated. In contrast, during PS treatment, it is expected that SiO_2 units formed on the acid sites located both on the internal and external surfaces of the crystal, leading to a decrease in acidic strength of the zeolite.

2.3. Characterization

The morphology and crystallinity of the obtained samples were analyzed using field emission scanning electron microscopy (FE-SEM; JSM-6500F, JEOL Co. Ltd.) and X-ray diffraction analysis (XRD; JDX-8020, JEOL Co. Ltd.), respectively. The surface areas of the obtained samples were calculated using the BET-method based on N_2 adsorption isotherms (Belsorp mini, BEL JAPAN Co. Ltd.). The Si/Al ratios of the samples were determined based on X-ray fluorescence measurements (XRF; Supermini, Rigaku Co. Ltd.), and the acidity of the obtained samples was evaluated using the ac-NH_3–TPD method [33]. In the TPD experiment, the carrier gas was 1.0% NH_3 (balance He), the heating rate was 5 K min^{-1}, and the temperature range was 373–823 K. The desorption of NH_3 molecules from the acid sites of the zeolite was measured under complete adsorption equilibrium conditions (1.0% NH_3–He atmosphere). Pyridine adsorption on the obtained samples was observed using a diffuse reflectance infrared Fourier transform (DRIFT) spectrometer equipped with a mercury cadmium telluride (MCT) detector (FT/IR-4100, JASCO Co. Ltd.). A total of 200 scans were averaged for each spectrum. Pre-treatment was conducted in vacuo at 723 K for 12 h, and then pyridine was introduced and adsorbed onto the sample at 373 K for 2 h. The physically adsorbed pyridine was then removed in flowing N_2 at 373 K for 0.5 h, and the remaining species were subsequently measured via Fourier transform infrared (FT-IR) analysis at 373 K.

2.4. Cumene and TIPB cracking

In order to evaluate the regioselective deactivation of the acid sites, the catalytic cracking of isopropyl benzene (cumene) and 1,3,5-triisopropyl benzene (TIPB) was carried out using a fixed-bed reactor at a reaction temperature of 573 K under an N_2 flow at atmospheric pressure [34,35]. The W/F ratio (W: amount of catalyst/g, F: feed rate/g h^{-1}) and the feed rate of cumene and TIPB were 0.13 h and 0.18 h, and 1.0 ml/h and 1.33 ml/h, respectively. The catalyst weight was 0.15 g. The composition of the exit gas was measured via on-line gas chromatography (GC-2014, Shimadzu Co. Ltd.) with a Unipak-S column for the FID detector.

2.5. ATO reaction

The ATO reaction over ZSM-5 zeolite catalysts was carried out using a fixed-bed reactor at a reaction temperature of 723 K under an N_2 flow at atmospheric pressure. The W/F ratio, feed rate of the acetone, and catalyst weight were 0.5 h, 1.8 ml/h, and 0.71 g, respectively. The composition of the exit gas was measured via on-line gas chromatography (GC-8A, Shimadzu Co. Ltd.) with a Porapak-Q column as the FID detector. The amount of coke deposited on the catalyst was determined via thermogravimetric analysis (TG; TGA-50, Shimadzu Co. Ltd.).

3. Results and discussion

3.1. Preparation of ZSM-5 zeolites with different crystal sizes

Fig. 1 shows X-ray diffraction patterns of samples obtained using conventional hydrothermal and emulsion preparation methods. The patterns of the samples contained peaks corresponding to MFI-type zeolites. Figs. 2 and 3 show FE-SEM micrographs and NH_3–TPD profiles of the obtained samples, respectively. As can be seen in Fig. 2, the crystal sizes of the macro- and nano-ZSM-5 zeolites were

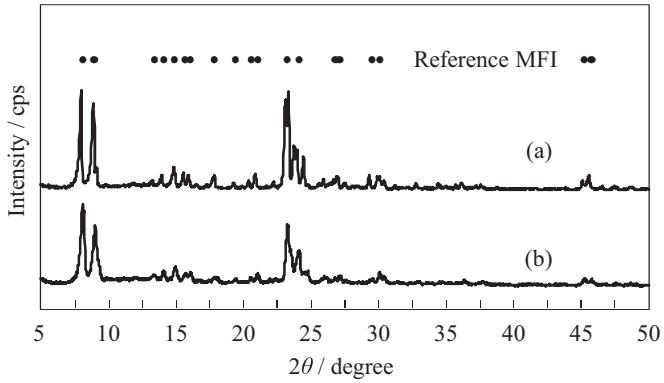

Fig. 1. XRD patterns of (a) macro- and (b) nano-ZSM-5 zeolites.

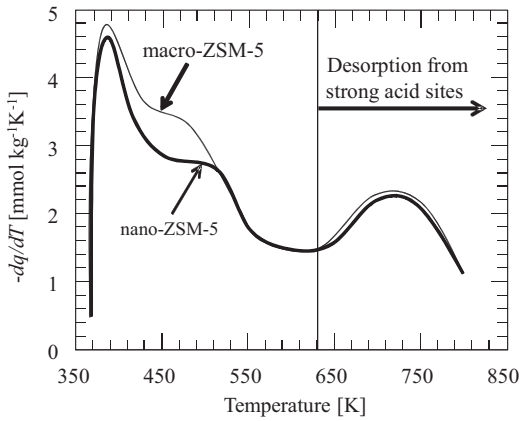

Fig. 3. NH_3–TPD profiles of macro- and nano-ZSM-5 zeolites.

approximately 1500 nm and 150 nm, respectively. In addition, as can be seen in Fig. 3, the ZSM-5 zeolites exhibited nearly the same amounts of strong acid sites regardless of the crystal size. Table 1 presents the Si/Al ratios determined via XRF and the surface areas of the obtained samples. Notably, the Si/Al ratios were nearly the same as the Si/Al ratio calculated from the Si and Al concentrations present in the synthetic solutions. Furthermore, the nano-ZSM-5 zeolite exhibited nearly the same BET surface area of 400 m^2/g as the macro-ZSM-5 zeolite. As a result, the macro- and nano-ZSM-5 zeolites with nearly the same types, strengths and concentrations of acid sites were obtained. Next, in order to investigate the effects of crystal size and the regioselective deactivation of the ZSM-5 zeolites on their catalytic performance, these zeolites were used as catalysts for the ATO reaction.

Table 1
BET surface areas and Si/Al ratios of macro- and nano-ZSM-5 zeolites.

Zeolite	S_{BET} ($m^2\ g^{-1}$)	$Si/Al_{measured\ by\ XRF}$
Untreated macro-ZSM-5	405	89
Untreated nano-ZSM-5	400	81
TPS-treated nano-ZSM-5	391	–
PS-treated nano-ZSM-5	370	–

3.2. Preparation of ZSM-5 zeolites with different acid site locations

Although the nano-ZSM-5 zeolite exhibited stable catalytic activity, the lifetime of this catalyst was insufficient and the product selectivity was unstable [21] due to the formation of coke on the external surface of the zeolite crystal and non-volatile carbonaceous compounds on the pore surfaces within the crystal. These compounds inhibit diffusion and adsorption of the reactant within the zeolite crystal. In order to overcome these problems, suppression of coke formation due to excessive reaction of the desired products is indispensable. Thus, the regioselective deactivation of acid sites located on the external surface of the zeolite crystal has been examined. One promising approach is the CCS (catalytic cracking of silane) method, which can achieve control and/or modification of the acidity of zeolites through the regioselective formation of SiO_2 units [28–30]. In this study, the CCS method was carried out using two different silanes: triphenyl silane (TPS) and phenyl silane (PS).

The FT-IR spectra of the adsorbed pyridine and ac-NH_3–TPD profiles of the nano-ZSM-5 zeolite before and after CCS treatment can be seen in Figs. 4 and 5, respectively. As shown in Fig. 4, the bands near 1450 and 1540 cm^{-1} are attributed to Lewis acid sites (LAS) and Brønsted acid sites (BAS), respectively [36]. Although the IR absorbance was qualitatively measured, it can be clearly seen that the intensity of the peaks corresponding to the acid sites decreased after CCS treatment. These changes in the acidity due to the CCS treatment could also be clearly observed in the NH_3–TPD profiles, as shown in Fig. 5. With both silane compounds, the amount of NH_3 desorbed from the acid sites (mainly BAS) decreased after CCS treatment due to the formation of SiO_2 units on the acid sites. In addition, the TPD profiles indicated that the quantity of acid sites for the PS-treated nano-ZSM-5 zeolite was less than that for the TPS-treated nano-ZSM-5 zeolite. The greater decrease in the amount of strong acid sites for the PS-treated nano-ZSM-5 zeolite is attributed to the relationship between the pore diameter of the ZSM-5 and the molecular size of the silane compound. In the case of TPS, because

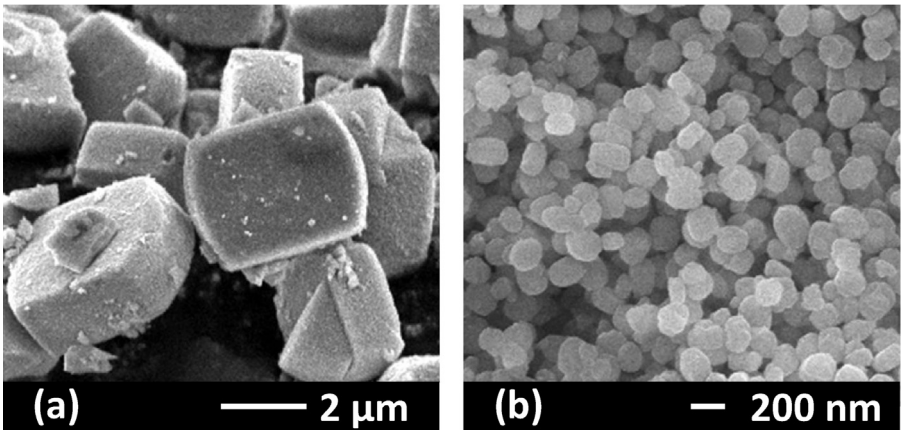

Fig. 2. SEM micrographs of (a) macro- and (b) nano-ZSM-5 zeolites.

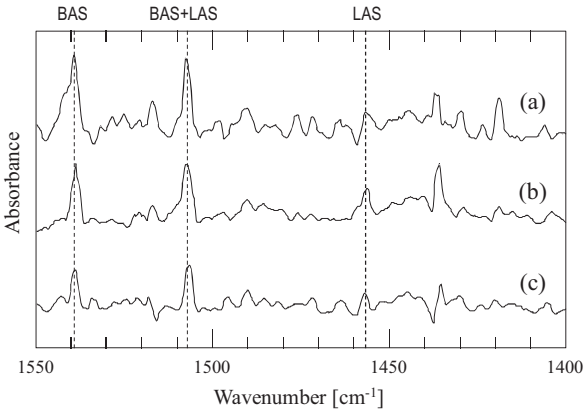

Fig. 4. FT-IR spectra of pyridine-adsorbed nano-ZSM-5 zeolites. (a) Before CCS treatment, (b) after TPS treatment, and (c) after PS treatment.

the molecular size of TPS is larger than the pore diameter of the ZSM-5, the acid sites located on the external surface were selectively deactivated. In contrast, because the molecular size of PS is slightly smaller than the pore diameter of the ZSM-5 zeolite, not only the acid sites on the external, but those on the internal surface were deactivated. Thus, the difference in the molecular size of these silane compounds influenced the number of acid sites that were deactivated, leading to the difference in the NH_3–TPD profiles.

During CCS treatment, because SiO_2 units are selectively formed only on the acid sites, the zeolitic pore properties, such as the pore size and surface, should remain nearly unchanged before and after treatment. In order to confirm this assumption, the N_2 adsorption and cracking activity for alkyl aromatics of nano-ZSM-5 zeolites before and after CCS treatment were examined. Fig. 6 shows the N_2 adsorption isotherms of nano-ZSM-5 zeolites before and after CCS treatment. As anticipated, the modified zeolites exhibited nearly the same micropore volume as the untreated nano-ZSM-5 zeolite. It can thus be concluded that the CCS method has an insignificant effect on the pore properties of zeolite catalysts.

3.3. Cumene and TIPB cracking over nano-ZSM-5 with different acid site locations

The results of cumene and TIPB cracking using nano-ZSM-5 with and without CCS treatment are presented in Fig. 7. In the cumene and TIPB cracking, it is well-known that these cracking reactions proceed on the Brønsted acid sites (not Lewis acid sites) [34,35]. The untreated nano-ZSM-5 (Fig. 7(a)) exhibited high catalytic activity for both reactions. In this case, however, the conversion of TIPB

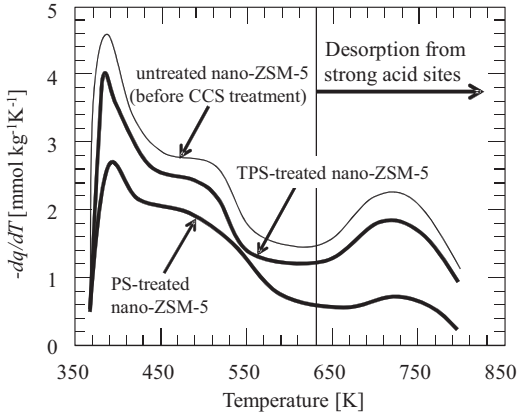

Fig. 5. NH_3–TPD profiles of the nano-ZSM-5 zeolites before/after CCS treatment.

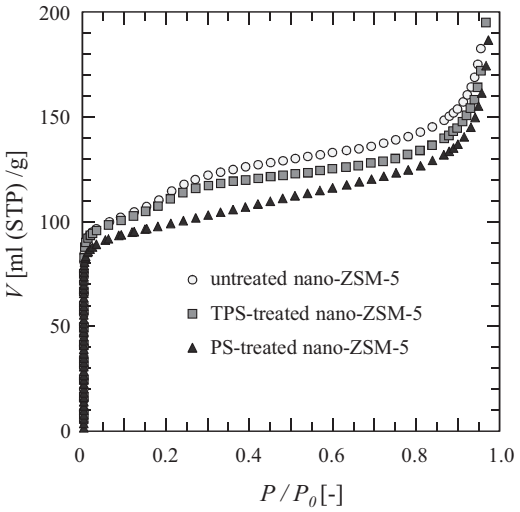

Fig. 6. N_2 adsorption isotherms of nano-ZSM-5 zeolites before/after CCS treatment.

gradually decreased with time on-stream, indicating that the external acid sites became poisoned due to coke formation [34,35].

The CCS-treated nano-ZSM-5 zeolites (Fig. 7(b) and (c)), on the other hand, showed almost no TIPB conversion despite having some intact acid sites, as confirmed by the high cumene conversion compared to the untreated ZSM-5 catalyst. The slight cracking of TIPB at the beginning of the reaction may be due to the very small number of acid sites remaining on the external of the zeolite. No additional

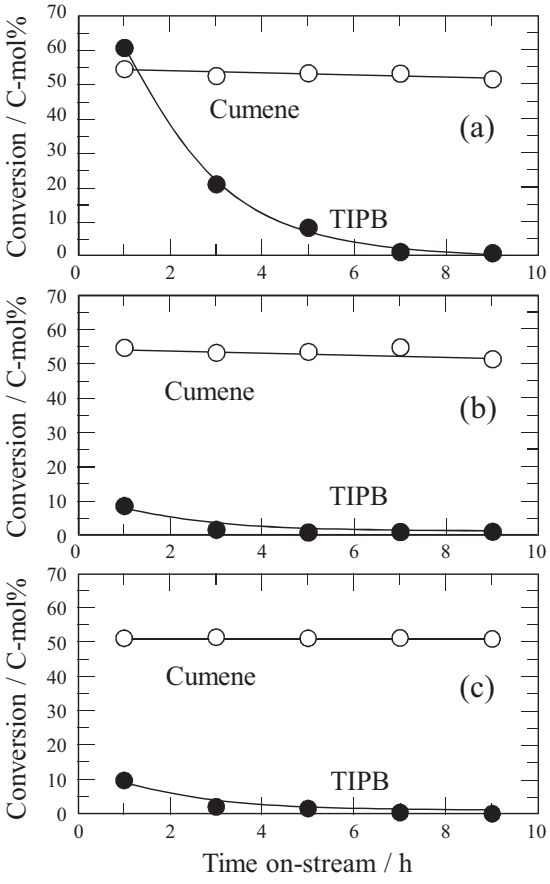

Fig. 7. Catalytic cracking results for isopropyl benzene (cumene) and 1,3,5-triisopropyl benzene (TIPB) over (a) untreated nano-ZSM-5, (b) TPS-treated nano-ZSM-5, and (c) PS-treated nano-ZSM-5 zeolites.

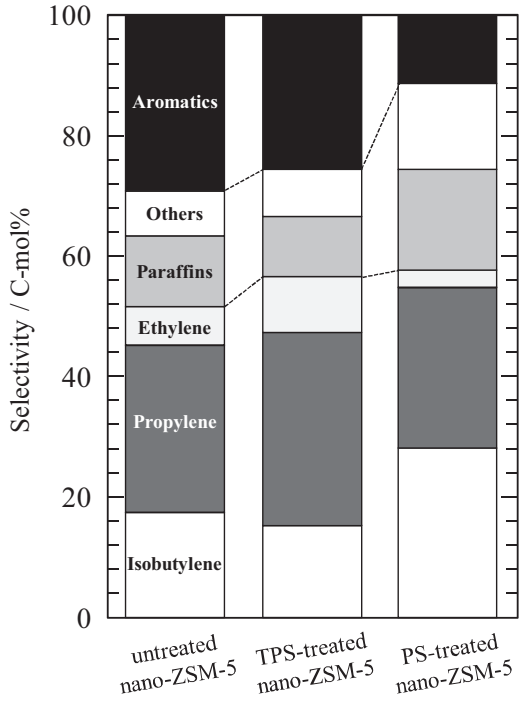

Fig. 8. Product selectivities after 2.5 h for reactions over nano-ZSM-5 with/without CCS treatment.

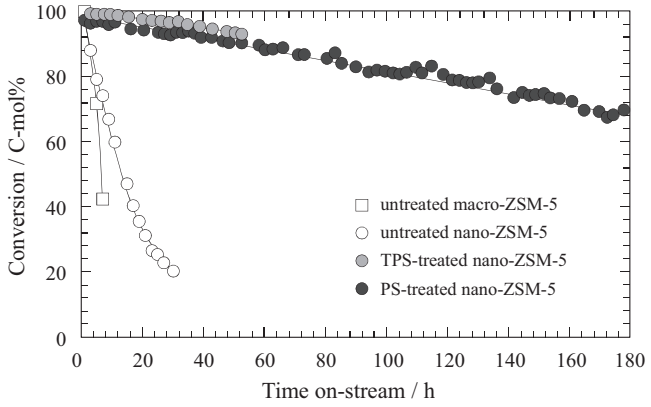

Fig. 9. Changes in acetone conversion with time on-stream over macro- and nano-ZSM-5 with/without PS treatment.

conversion of TIPB was observed, however, indicating that the complete deactivation of the external acid sites was readily accomplished by the slight coke deposition that occurred during TIPB cracking at the initial stage of the reaction. These results strongly imply that the Brønsted acid sites on the external surface of nano-ZSM-5 catalysts are selectively deactivated after CCS treatment. In contrast, the ZSM-5 zeolites after CCS treatment exhibited an activity for cumene cracking as high as the untreated nano-ZSM-5. The high catalytic activity for cumene suggests that the cumene diffused into the channels of the CCS-treated ZSM-5-zeolites, which in turn indicates that the pore size of the ZSM-5 zeolites were largely unchanged after CCS treatment, because the minimum molecular diameter of cumene, which corresponds to the diameter of a benzene ring, is nearly the same as the pore diameter of untreated ZSM-5 zeolite. Notably, the initial cumene conversion for the PS-treated nano-ZSM-5 (51 C-mol%) was slightly lower than that for the TPS-treated nano-ZSM-5 (55 C-mol%), indicating that more SiO_2 units were formed on the Brønsted acid sites located on the internal and external surfaces of the PS-treated crystal, but a sufficient number of the Brønsted acid sites remained on the internal surface to the catalytic reaction. Next, to further investigate the effects of the CCS treatment on catalytic performance, these modified nano-ZSM-5 zeolites were used as catalysts for the ATO reaction.

3.4. Catalytic performance of ZSM-5 zeolites with different acid site locations

In the ATO reaction, isobutylene is first produced as an aldol condensation product of acetone, and then converted to propylene, ethylene, and aromatics over the acid sites. These light olefins are intermediate chemicals in a series of reactions that ends with the production of aromatics and coke. The product selectivities and acetone conversions shortly after initiation of the reaction (2.5 h) over the nano-ZSM-5 zeolites with and without CCS treatment are shown in Fig. 8. CCS treatment of the nano-zeolite improved the light olefin selectivity (TPS: 57 C-mol%, PS: 58 C-mol%) and suppressed aromatics formation (TPS: 26 C-mol%, PS: 11 C-mol%) compared with that of the nano-ZSM-5 zeolite before CCS treatment (light olefins: 52 C-mol%, aromatics: 29 C-mol%). The improvement in the light olefins selectivity is ascribed to the suppression of non-selective and excessive reactions producing aromatics. After TPS-treatment, high ethylene and propylene yields were obtained because the generated isobutylene reacted with itself to produce ethylene and propylene via dimerization/cracking over the acid sites inside the zeolite crystal, where strong acidity remained. In contrast, with the PS-treated catalyst, both a high isobutylene yield and significantly reduced aromatic selectivity were achieved. After PS treatment, in addition to the acid sites on the external surface of the zeolite, the acid sites in the cross-sectional spaces inside the zeolite crystal, which are wide open spaces, were also deactivated. Accordingly, it is considered that SiO_2 formation on both the external surface and the internal pore surfaces led to the suppression of the dimerization and cyclization of isobutylene and subsequent formation of aromatics and coke. As a result, both CCS-treated nano-ZSM-5 zeolites were effective catalysts for the production of light olefins at high yield. Furthermore, regioselective deactivation of the acid sites was achieved using the CCS method with silane compounds with different molecular sizes, leading to control of zeolite acidity and consequently the product selectivity of the catalysts.

Fig. 9 shows the changes in acetone conversion with time on-stream over the ZSM-5 zeolites with and without CCS treatment. Although the untreated nano-ZSM-5 catalyst exhibited stable activity compared to that of the macro-ZSM-5 zeolite, the conversion decreased to 20 C-mol% after 30 h. In contrast, the TPS-treated and PS-treated nano-ZSM-5 maintained a high conversions above 93% for 50 h and 70% for 180 h, respectively. This result indicates excellent stability compared to that of the ZSM-5 zeolite without CCS treatment. The amounts of coke formed on the catalysts as measured by TG analysis are listed in Table 2. Although the reaction time of the nano-ZSM-5 zeolite after CCS treatment using PS was much longer than that of the nano-ZSM-5 catalyst without CCS treatment, the amount of coke formed on the PS-treated nano-ZSM-5 zeolite after the reaction (9.0 wt% after 180 h) was comparable to that of the macro- and nano-ZSM-5 catalysts before CCS treatment (macro-ZSM-5: 8.5 wt% after 6.5 h; nano-ZSM-5: 8.2 wt% after 30 h).

Table 2
Amount of coke produced using ZSM-5 zeolite catalysts as determined by TG analysis.

Zeolite	Reaction time (h)	Coke amount (wt%)
Untreated macro-ZSM-5	6.5	8.5
Untreated nano-ZSM-5	30.0	8.2
PS-treated nano-ZSM-5	180.0	9.0

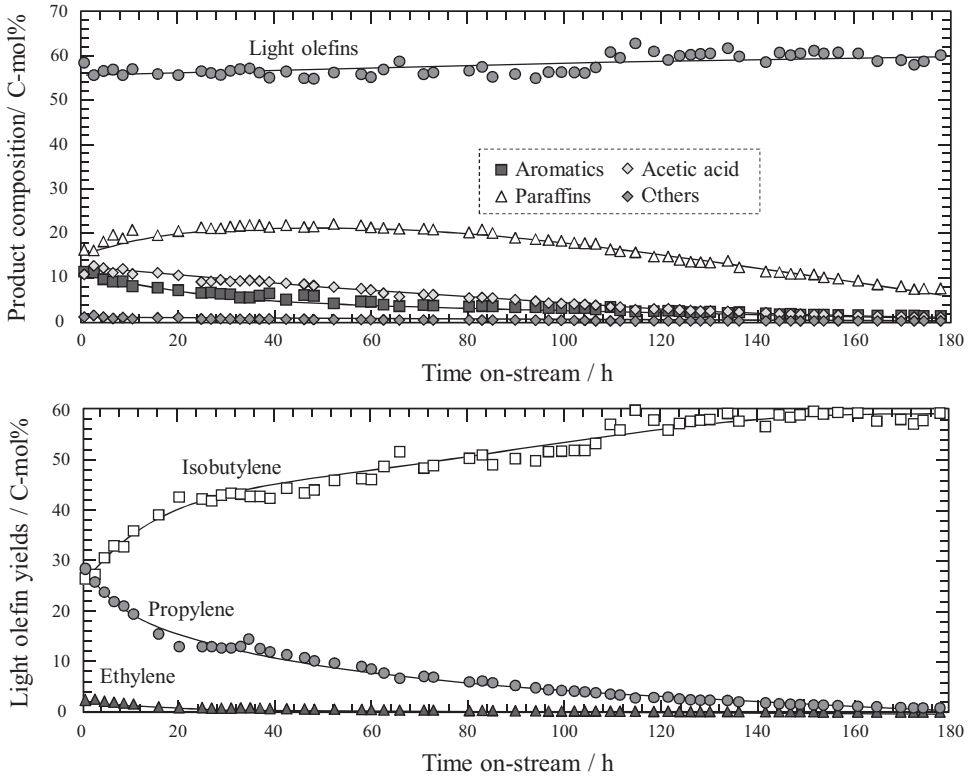

Fig. 10. Product yields with time on-stream over the PS-treated nano-ZSM-5 zeolite.

Thus, the CCS treatment enabled the suppression of coke formation, leading to the excellent stability.

Finally, Fig. 10 shows the product yields over the PS-treated nano-ZSM-5 catalyst. It is apparent that the high yield of light olefins (particularly isobutylene) was maintained for a long reaction time (180 h), and that this catalyst exhibited remarkable catalytic performance compared to that observed in our previous study [21,22]. The isobutylene yield was increased with time-on stream. This is because the consecutive reactions were suppressed along with the decrease in the acidity due to coke formation. In the ATO reaction, isobutylene was first produced from acetone, followed by production of propylene, ethylene, and aromatics. These intermediates are involved in a series of reactions that result in the generation of coke as the terminal product. In this reaction, the consecutive reactions were suppressed along with the decrease in the acid amounts due to CCS treatment and coke formation. Fig. 11 summarizes the relationship between acetone conversion and light olefins yield in the ATO reaction over macro- and nano-ZSM-5 zeolites before/after CCS treatment. The CCS-treated nano-ZSM-5 was exhibited high light olefins yield as compared with untreated ZSM-5 zeolites. Therefore, it is believed that the CCS treatment is effective for improving the light olefins yield. From these results, it can be concluded that the modification of nano-ZSM-5 zeolites using the CCS method is effective for improving the isobutylene yield and catalytic stability when these zeolites are used as catalysts for the ATO reaction.

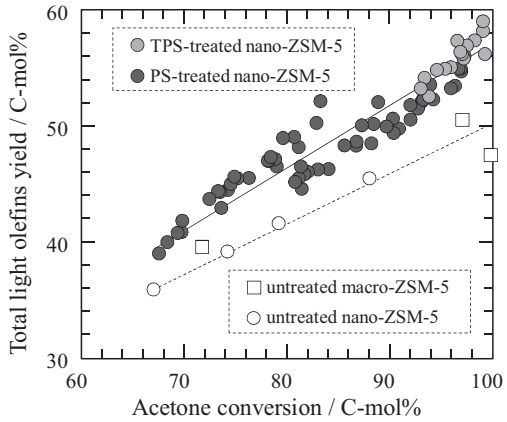

Fig. 11. Relationship between acetone conversion and light olefins yield.

4. Conclusion

The regioselective deactivation of the acid sites on nano-ZSM-5 zeolites was achieved using the CCS method with silane compounds of different molecular sizes, leading to the control of the zeolite acidity. These modified nano-ZSM-5 zeolites were then applied as catalysts for the ATO reaction, and the regioselective deactivation of the acid sites due to CCS treatment resulted in remarkable catalytic performance. In particular, the PS-treated nano-ZSM-5 zeolite exhibited a high yield of light olefins with excellent stability compared to the results obtained with the macro- and nano-ZSM-5 zeolites without CCS treatment.

Acknowledgements

This work was supported by a Research Grant Program of the New Energy and Industrial Technology Development Organization (NEDO) of Japan and the Global COE Program (Project No. B01: Catalysis as the Basis for Innovation in Materials Science) from the Ministry of Education, Culture, Sports, Science and Technology, Japan.

References

[1] Y. Yoshimura, N. Kijima, T. Hayakawa, K. Murata, K. Suzuki, F. Mizukami, K. Matano, T. Konishi, T. Oikawa, M. Saito, T. Shiojima, K. Shiozawa, K. Wakui, G. Sawada, K. Sato, S. Matsuo, N. Yamaoka, Catal. Surv. Jpn. 4 (2000) 157–167.
[2] O. Bortnovsky, P. Sazama, B. Wichterlova, Appl. Catal. A: Gen. 287 (2005) 203–213.
[3] C. Mei, P. Wen, Z. Liu, Y. Wang, W. Yang, Z. Xie, W. Hua, Z. Gao, J. Catal. 258 (2008) 243–249.
[4] A. Corma, J. Planelles, J. Sanchezmarin, F. Tomas, J. Catal. 93 (1985) 30–37.
[5] S.M. Babitz, B.A. Williams, J.T. Miller, R.Q. Snurr, W.O. Haag, H.H. Kung, Appl. Catal. A: Gen. 179 (1999) 71–86.
[6] H. Mochizuki, T. Yokoi, H. Imai, R. Watanabe, S. Namba, J.N. Kondo, T. Tatsumi, Micropor. Mesopor. Mater. 145 (2011) 165–171.
[7] K. Kubo, H. Iida, S. Namba, A. Igarashi, Micropor. Mesopor. Mater. 149 (2012) 126–133.
[8] S. Inagaki, S. Shinada, Y. Kaneko, K. Takechi, R. Komatsu, Y. Tsuboi, H. Yamazaki, J.N. Kondo, Y. Kubota, ACS Catal. 3 (2013) 74–78.
[9] H. Konno, T. Okamura, Y. Nakasaka, T. Tago, T. Masuda, J. Jpn. Petrol. Inst. 55 (2012) 267–274.
[10] H. Konno, T. Okamura, Y. Nakasaka, T. Tago, T. Masuda, Chem. Eng. J. 207–208 (2012) 460–467.
[11] H. Konno, T. Tago, Y. Nakasaka, R. Ohnaka, J. Nishimura, T. Masuda, Micropor. Mesopor. Mater. 175 (2013) 25–33.
[12] M. Stocker, Micropor. Mesopor. Mater. 29 (1999) 3–48.
[13] F.J. Keil, Micropor. Mesopor. Mater. 29 (1999) 49–66.
[14] Y. Kumita, J. Gascon, E. Stavitski, J.A. Moulijn, F. Kapteijn, Appl. Catal. A: Gen. 391 (2011) 234–243.
[15] T. Meng, D. Mao, Q. Guo, G. Lu, Catal. Commun. 21 (2012) 52–57.
[16] Y. Furumoto, Y. Harada, N. Tsunoji, A. Takahashi, T. Fujitani, Y. Ide, M. Sadakane, T. Sano, Appl. Catal. A: Gen. 399 (2011) 262–267.
[17] D. Goto, Y. Harada, Y. Furumoto, A. Takahashi, T. Fujitani, Y. Oumi, M. Sadakane, T. Sano, Appl. Catal. A: Gen. 383 (2010) 89–95.
[18] C. Yu, Q. Ge, H. Xu, W. Li, Appl. Catal. A: Gen. 315 (2006) 58–67.
[19] L. Liu, Q. Deng, Y. Liu, T. Ren, Z. Yuan, Catal. Commun. 16 (2011) 81–85.
[20] R.J. Schmidt, Appl. Catal. A: Gen. 280 (2005) 89–103.
[21] T. Tago, H. Konno, M. Sakamoto, Y. Nakasaka, T. Masuda, Appl. Catal. A: Gen 403 (2011) 183–191.
[22] T. Tago, H. Konno, S. Ikeda, S. Yamazaki, W. Ninomiya, Y. Nakasaka, T. Masuda, Catal. Today 164 (2011) 158–162.
[23] S.H. McAllister, W.A. Bailey, C.M. Bouton, J. Am. Chem. Soc. 62 (1940) 3210–3215.
[24] J. Cejka, L. Kubelkova, P. Jiru, Collect. Czech. Chem. Commun. 54 (1989) 2054–2062.
[25] J. Cejka, P. Jiru, Collect. Czech. Chem. Commun. 54 (1989) 2998–3002.
[26] L. Kubelkova, J. Cejka, J. Novakova, Zeolite 11 (1991) 48–53.
[27] A.G. Panov, J.J. Fripiat, J. Catal. 178 (1998) 188–197.
[28] T. Tago, K. Iwakai, K. Morita, K. Tanaka, T. Masuda, Catal. Today 105 (2005) 662–666.
[29] T. Tago, M. Sakamoto, K. Iwakai, H. Nishihara, S.R. Mukai, T. Tanaka, T. Masuda, J. Chem. Eng. Jpn. 42 (2009) 162–167.
[30] T. Masuda, N. Fukumoto, M. Kitamura, S.R. Mukai, K. Hashimoto, T. Tanaka, T. Funabiki, Micropor. Mesopor. Mater. 48 (2001) 39–245.
[31] T. Tago, M. Nishi, Y. Kouno, T. Masuda, Chem. Lett. 33 (2004) 1040–1041.
[32] T. Tago, H. Konno, Y. Nakasaka, T. Masuda, Catal. Surv. Asia 16 (2012) 148–163.
[33] T. Masuda, Y. Fujikata, S.R. Mukai, K. Hashimoto, Appl. Catal. A: Gen. 165 (1997) 57–72.
[34] C. Anand, I. Toyama, H. Tamada, S. Tawada, S. Noda, K. Komura, Y. Kubota, S.W. Lee, S.J. Cho, J.H. Kim, G. Seo, A. Vinu, Y. Sugi, Ind. Eng. Chem. Res. 51 (2012) 12214–12221.
[35] S. Inagaki, S. Shinoda, Y. Kaneko, K. Takechi, R. Komatsu, Y. Tsuboi, H. Yamazaki, J.N. Kondo, Y. Kubota, ACS Catal. 3 (2013) 74–78.
[36] E.P. Parry, J. Catal. 2 (1963) 371–379.